View metadata, citation and similar papers at core.ac.uk

brought to you by CORE

provided by IntechOpen

We are IntechOpen, the world's leading publisher of Open Access books Built by scientists, for scientists

4,800
Open access books available

122,000
International authors and editors

135M
Downloads

Our authors are among the

154
Countries delivered to

TOP 1%
most cited scientists

12.2%
Contributors from top 500 universities

CLARIVATE ANALYTICS BOOK CITATION INDEX INDEXED

WEB OF SCIENCE™

Selection of our books indexed in the Book Citation Index in Web of Science™ Core Collection (BKCI)

Interested in publishing with us?
Contact book.department@intechopen.com

Numbers displayed above are based on latest data collected.
For more information visit www.intechopen.com

3

A Tunable Semiconductor Lased Based on Etched Slots Suitable for Monolithic Integration

D. C. Byrne, W. H. Guo, Q. Lu and J. F. Donegan
School of Physics, Trinity College Dublin
Ireland

1. Introduction

Widely tunable semiconductor lasers will play a critical part in future technologies. Tunable lasers are rapidly replacing fixed wavelength lasers in dense wavelength division multiplexing DWDM optical communications. The performance specifications of tunable lasers are the same as fixed wavelength specifications plus additional specifications that include: wavelength tuning range; wavelength switching speed; and minimum wavelength spacing. Tunable lasers diodes (TLD) have been used in optical networks for some time now starting with devices with small wavelength coverage and moving towards full band coverage.

Wavelength-agile networks are also simplified with tunable lasers. Reconfigurable optical add–drop multiplexers (ROADMs) and wavelength-based routing enable service providers to offer differentiated services, meet the ever-increasing demand for bandwidth and deliver all-optical networking. Tunable lasers are key to addressing this growing need to reconfigure networks remotely. The use of widely tunable lasers helps maximize existing network resources. The ability to dynamically provision bandwidth provides the ability to optimize the network configuration to meet demand. Widely tunable lasers move traffic from overcrowded channels to unused channels and are becoming essential for the network architecture.

Future DWDM networks will make more use of wavelength converters to increase network flexibility. Wavelength converters, such as, optical-electronic-optical (OEO) converters with the ability to detect a high data rate signal on any input wavelength channel and to convert to any output wavelength channel, will use tunable lasers. Future uses for tunable lasers will also include packet based selection of the wavelength on which the packet is to be transmitted. The tunable laser switching speed for these applications will be of the order of micro-seconds or longer. They will typically need to be widely tunable, i.e. tunable over a full C or L band and should be tunable to the 50 GHz channel spacing. In some UDWDM applications, channel spacing of 25 GHz and eventually as close as 12.5 GHz will be required.

Tunable lasers will also be used as a means to reduce costs as sparing lasers in wavelength division multiplexing (WDM) systems. New approaches to data transmission such as coherent WDM (CoWDM (Healy, Garcia Gunning et al. 2007)) require discrete tuning between particular wavelength channels on a grid. There is additionally an urgent need to integrate semiconductor lasers with other optical components such as amplifiers,

Source: Advances in Optical and Photonic Devices, Book edited by: Ki Young Kim,
ISBN 978-953-7619-76-3, pp. 352, January 2010, INTECH, Croatia, downloaded from SCIYO.COM

modulators and detectors (Coldren 2000; Ward, Robbins et al. 2005; Welch, Kish et al. 2006; Raring & Coldren 2007) in order to reduce chip cost, system size and complexity. Tunable lasers are also needed in other important markets such as trace gas detection for environmental emission motoring (Phelan, Lynch et al. 2005).

Laser operation requires optical feedback which is conventionally obtained in a semiconductor Fabry-Pérot laser by cleaving the ends of the laser waveguide along either (011) or (01-1) crystallographic planes to form two semi-reflecting facets. However, due to the need for cleaving, it is difficult to integrate these lasers with other optical components on a single chip.

Distributed-Bragg-reflector (DBR) lasers and distributed feedback (DFB) lasers which employ a series of small refractive-index perturbations to provide feedback, do not rely on cleaved facets and therefore can be integrated with optical amplifiers and modulators.

However, complex processing with multiple epitaxial growth stages is required for fabricating these lasers. Another method to obtain feedback is to etch a facet. However, this approach is limited by difficulties in achieving the smoothness and verticality of the etched facet particularly for structures based on InP materials.

Previously it was shown that by introducing a shallow slot into the active ridge waveguide of a laser, the longitudinal modes of the Fabry-Perot (FP) cavity were perturbed according to the position of the slot with respect to the cleaved facets (Coldren & Koch 1984; Peters & Cassidy 1991; Corbett & McDonald 1995). By judicious placement of a sequence of low-loss slots with respect to the facets pre-selected FP modes could be significantly enhanced leading to robust single frequency lasing with wide temperature stability (John, Dewi et al. 2005; O'Brien & O'Reilly 2005) as well as tuning with fast switching characteristics (Phelan, Wei-Hua et al. 2008). More recently, we have characterized the properties of slots which are etched more deeply namely to the depth of, but not through, the core waveguide containing the quantum wells (Roycroft, Lambkin et al. 2007). In that case, the reflection of each slot is of the order of ~1% with transmission of ~80% and the slot will strongly perturb the mode spectrum of the FP cavity by creating sub-cavities. The loss introduced by the presence of the slot is compensated by gain in the laser. An array of such slots can provide the necessary reflectivity for the laser operation independent of a cleaved facet where the gain between the slots compensates for the slot loss producing an active slotted mirror region. Such a mirror has been used in conjunction with a cleaved facet permitting the integration of a photodetector with the laser. As the laser output facet is not cleaved this can provide a much easier integration platform on which complex devices such as Mach-Zehnder modulators (MZI) and semiconductor optical amplifiers (SOA) can be monolithically integrated with the laser to reduce chip cost and complexity significantly. In this chapter we demonstrate a tunable laser with an integrated SOA which is used to both increase and balance the output optical power of different channels.

2. Background on slot design

In this section a single slotted Fabry-Perot laser diode will be introduced which forms the basis for our tunable platform. The single slot laser is fabricated by etching into the waveguide of the FP laser diode as described in (DeChiaro 1991; McDonald & Corbett 1996; Fessant & Boucher 1998; Klehr, Beister et al. 2001; Lambkin, Percival et al. 2004; Engelstaedter, Roycroft et al. 2008). The slots act as reflection centres and produce a modulation of the reflection and transmission spectra dependent on the characteristics of the

slot such as slot position, slot depth to which it is etched and slot width. Even though the slot is not etched into the active (waveguiding) regions it will still interact with the mode of the electric field (and magnetic field) of the waveguide as the mode profile is not fully confined to the active region and will expand into the surrounding cladding regions. The one-dimensional first order electric field mode profile modelled using the finite difference time domain (FDTD) technique for a simple laser structure with active region depth of 1 μm, upper cladding region of 1 μm and lower cladding of 1 μm with active region refractive index of 3.55 and cladding region refractive index 3.41, which are normal values for an InGaAsP active region sandwiched between InP cladding regions, are shown below in Fig. 1.

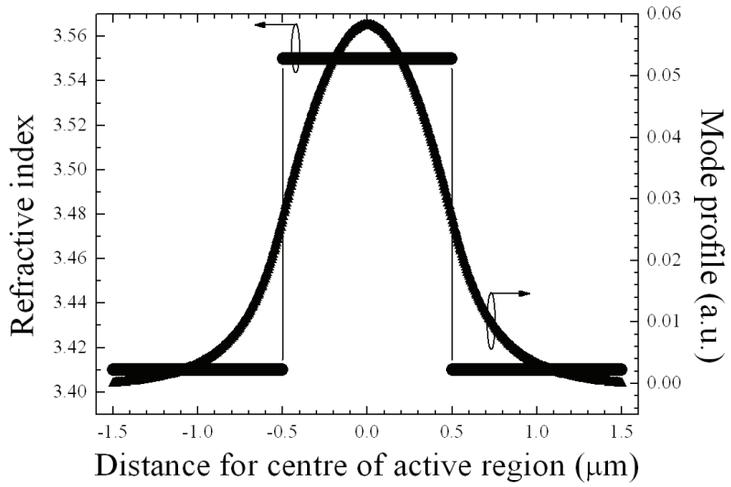

Fig. 1. Mode profile of the fundamental mode and refractive index profile through the laser structure.

From Fig. 1 the fundamental mode is seen to penetrate into the cladding region so any perturbation in this area will influence the mode profile of the laser diode.
The scattering matrix method (SMM) is a simple and accurate technique which can be used to determine the reflection and transmission from slots etched into the laser cavity. Numerous texts deal with the SMM of which (Buus, Amann et al. 2005) is a good introduction. Of particular importance in a laser structure is the ability to determine loss using the SMM method. This is an important advantage of the SMM over that transmission matrix method (TMM). A F-P laser with one etched slot can be described as three cavities with different interface reflections and transmissions as described below in Fig 2.

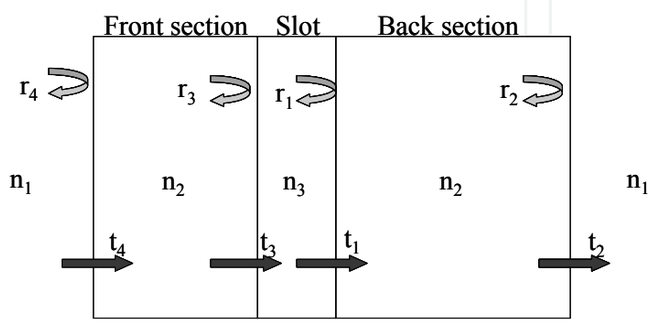

Fig. 2. Schematic description of single slot laser diode.

In fig. 2, n_i refers to the effective refractive index in these section of the laser structure, while r_i refers to the reflection from the interfaces as shown above. Each section can be described as a separated cavity and the total reflection and transmission is then found. The back section amplitude reflection from the left side and right side is described from the SMM as

$$r_{bl} = r_1 + \frac{t_1 r_2 \left(-t_1\right) \exp\left(-2i\tilde{\beta}_b L_b\right)}{1 - r_2 \left(-r_1\right) \exp\left(-2i\tilde{\beta}_b L_b\right)} \tag{1}$$

and

$$r_{br} = -r_2 + \frac{t_2 \left(-r_1\right)\left(-t_2\right) \exp\left(-2i\tilde{\beta}_b L_b\right)}{1 - r_2 \left(-r_1\right) \exp\left(-2i\tilde{\beta}_b L_b\right)} \tag{2}$$

respectively where $\tilde{\beta}$ is the complex propagation constant ($\tilde{\beta} = \beta_{re} + i\beta_{im}$) and L_b is the back section cavity length. The back section amplitude transmission from the left side is described as

$$t_{bl} = \frac{t_1 t_2 \exp\left(-i\tilde{\beta}_b L_b\right)}{1 - r_2 \left(-r_1\right) \exp\left(-2i\tilde{\beta}_b L_b\right)} \tag{3}$$

and

$$t_{br} = t_{bl}$$

giving a power reflection and transmission is $R_{bl} = (r_{bl})^2$ and $T_{br} = (t_{br})^2$ respectively. The reflection and transmission of the back section and slot region is found by including the back section reflection and transmission in the SMM calculation as follows

$$r_{bl+sl} = r_3 + \frac{t_3 r_{bl} \left(-t3\right) \exp\left(-2i\tilde{\beta}_s L_s\right)}{1 - r_{bl} \left(-r_3\right) \exp\left(-2i\tilde{\beta}_s L_s\right)} \tag{4}$$

and

$$t_{bl+sl} = \frac{t_3 t_{bl} \exp\left(-i\tilde{\beta}_b L_b\right)}{1 - r_{bl} \left(-r_3\right) \exp\left(-2i\tilde{\beta}_s L_s\right)} \tag{5}$$

again by a continuation of this method the reflection and transmission amplitudes for the full laser structure can be determined as

$$r_{totall} = r_4 + \frac{t_4 r_{bl+sl} \left(-t_4\right) \exp\left(-2i\tilde{\beta}_f L_f\right)}{1 - r_{bl+sl} \left(-r_4\right) \exp\left(-2i\tilde{\beta}_f L_f\right)} \tag{6}$$

and

$$t_{totall} = \frac{t_4 t_{bl+sl} \exp\left(-i\tilde{\beta}_f L_f\right)}{1 - r_{bl+sl} \left(-r_4\right) \exp\left(-2i\tilde{\beta}_f L_f\right)} \tag{7}$$

where the reflection and transmission from the right is found in a similar fashion to the total from the left. The calculated power reflection using an experimentally determined gain profile is shown in Fig. 3.

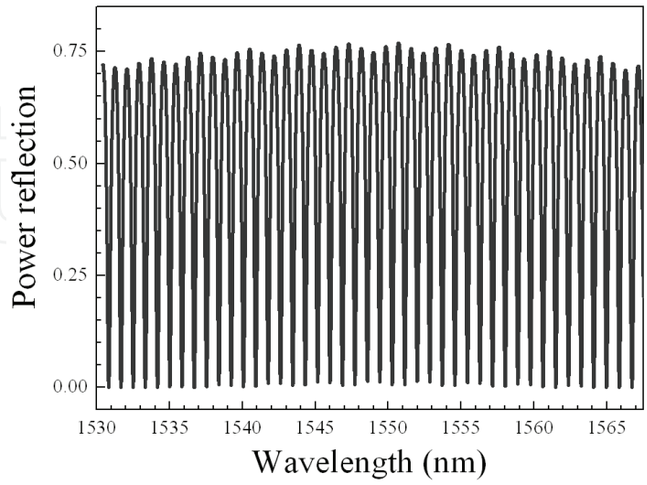

Fig. 3. Calculated reflection spectrum of a single slot laser diode versus wavelength operating near 1550 nm.

A modulation of the Fabry-Pérot modes is observed due to the slot. The strength and position of the modulation is dependent on the depth to which the slots are etched and the position of the slots in the laser cavity. An experimentally measured output spectrum recorded on an optical spectrum analyser (OSA) of a single slot laser diode with cleaved facets and a total cavity length of 350 μm and a slot position of 100 μm from the output facet is shown in Fig. 4. Coupled output power refers to the amount of output light collected by the measurement system.

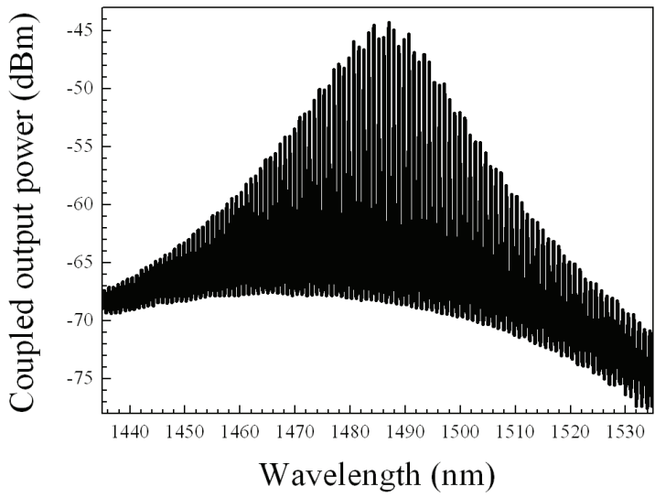

Fig. 4. Coupled output spectrum of single slot laser diode.

From the output spectrum the position of the slot can be determined by using a Fourier transform (FT) on the spectrum. The FT is calculated by the method described in (Guo,

Qiao-Yin et al. 2004) with the described deconvolution to remove the finite bandwidth resolution of the OSA. The FT spectrum is shown in Fig. 5 below.

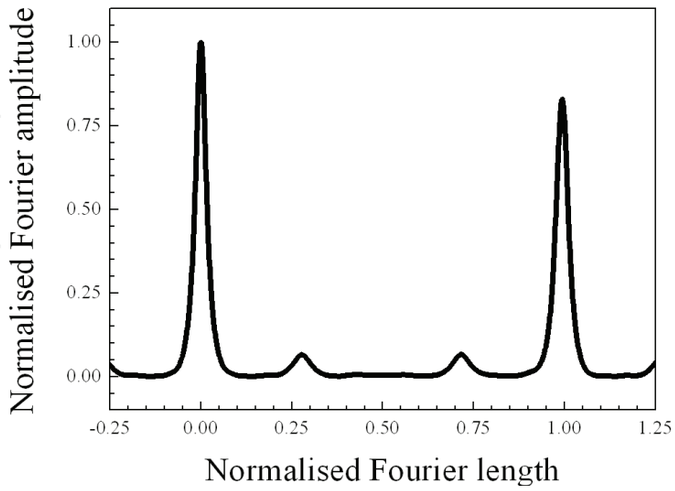

Fig. 5. Fourier transformed single slot spectrum, the large peaks at 0 and 1 are the facet reflection and harmonic while the two small peaks are the slot position and harmonic.

The single slot laser described here gives some mode selectivity however for single longitudinal mode operation more slots are needed and for a widely tunable laser multiple slot sections are included and the Vernier tuning method is utilised.

3. Electronic wavelength control

In order to have control of the output wavelength of a tunable laser diode we need to control the position of the gain peak wavelength of the cavity round trip gain (λ_p) and/or the longitudinal modes (λ_i). The gain peak wavelength (λ_p) is dependent on the injected carrier density however as the carrier density clamps above threshold widely tunable laser diodes cannot relay on this mechanism for large wavelength tuning.
Therefore in order to shift the output wavelength we need to change the positions of the longitudinal modes (λ_i) by changing the real part of the effective refractive as seen in the phase condition below (8),

$$\lambda_i = \frac{2n'_{eff}(\lambda_i)L}{m} \tag{8}$$

where n'_{eff} is the effective refractive index, L is the cavity length and m is the mode number. Therefore to control the output wavelength we need a waveguide with an electronically controllable effective refractive index where the amount of tuning is proportional to the product of the cavity length and the effective refractive index. With simple Fabry-Pérot laser diodes this provides little tuning of the output wavelength (a few nm) and so we look again at DBR and DFB type lasers. In DBR and DFB lasers the tuning of the cavity round-trip gain may be accomplished by tuning the Bragg reflector hence changing the position of the comb modes. Looking at equation (9)

$$\Lambda = \frac{\lambda_B}{2n'_{eff}} \tag{9}$$

we see that the only element that can be changed is the effective refractive index as the grating element is fixed during the fabrication of the Bragg mirror. As the effective refractive index is determined by the confinement factor and the refractive index of the layers of the laser diode any changes in the refractive index in any of these layers can change the effective refractive index and therefore the mirror loss $\alpha_m(\lambda)$. This type of tuning is employed commonly in many tunable laser diodes.

The extent of the lasers continuous tuning when the same cavity mode lases across the wavelength span can be determined easily form (10)

$$\frac{\Delta\lambda}{\lambda_0} = \frac{\left|\Delta n'_{eff}\right|}{n_{g,eff}} \tag{10}$$

where $\Delta\lambda$ is the wavelength tuning, λ_0 is the Bragg wavelength Δ'_{eff} is the change in the real part of the effective refractive index and $n_{g,eff}$ is the group effective refractive index. Allowing for mode hops between different longitudinal modes (discontinuous tuning) then the maximum tuning range is dependent on the spectral width of the gain envelope function. From this analysis we see that the electronic control of the wavelength of a tunable laser diode is dependent on our ability to control the effective refractive index of the laser. The effective refractive index may be controlled in practice by three different methods either carrier induced effects (free carrier plasma effect), by applying an electric across the device however this needs a reversed biased section(quantum confined Stark effect) or by varying the temperature of the device (thermal tuning).

DBR and DFB type laser diodes can be tuned by either changing the injected current or changing the temperature, however there is a limit to the tunability achieved by these methods (5-10 nm using refractive index changes) due to a limit in how much the refractive index or electronic bandgap can be changed. The gain bandwidth available to multiple quantum well lasers is ~ 100 nm and Erbium Doped Fibre Amplifiers (EDFA) have access to ~ 40 nm in the C or L band. Therefore there has been a large amount of research in extending the tunability of laser diodes beyond the refractive index limit (Jayaraman, Chuang et al. 1993; Rigole, Nilsson et al. 1995).

Increases in tunability can be obtained by using coupled cavities or array waveguide lasers which are discussed below however, these induce large complexities into the laser design and growth. In order to increase the tunability further we use a technique that allows us to use the change in the refractive index difference instead of the refractive index itself, therefore allowing a relative wavelength change to be used which can be much larger that the wavelength change due to a refractive index change. One method that exploits this relative refractive difference of semiconductor lasers is the Vernier effect. This effect requires two differing wavelength dependent mirror reflectivities to produce two spectrally different comb mode reflection spectra. The comb mode reflection spectra peaks will overlap at certain wavelengths which will produce lasing as at these wavelengths the gain will overcome loss since the round-trip loss is inversely proportional to the product of both mirror reflectivities. Both mirror reflection spectra can be directly and independently controlled by controlling the effective refractive index in these mirror regions. Any change

in the effective refractive index in the mirror regions will produce a shift in the comb mode reflection spectra and allow different reflection peaks to overlap shifting the wavelength accordingly. This idea of Vernier tuning the output wavelength is shown in Fig. 6. This method can greatly increase the tuning range and lasers such as the Sample Grating Distributed Bragg Reflector (SGDBR) laser which have recorded tuning ranges of ever 60 nm (Oku, Kondo et al. 1998; Mason, Fish et al. 2000), however some limitations apply to this kind of tuning which are:

- If two modes are overlapped and on the gain curve some other means of suppressing the unwanted mode must be employed to preserve a high side mode suppression ratio (SMSR) which is a measure of the quality of the single mode of the laser.
- There must be large enough cavity gain to suppress other competing modes.
- To achieve continuous tuning there must be a phase control element meaning that the round trip phase must be controlled to be an integer multiple of 2π.

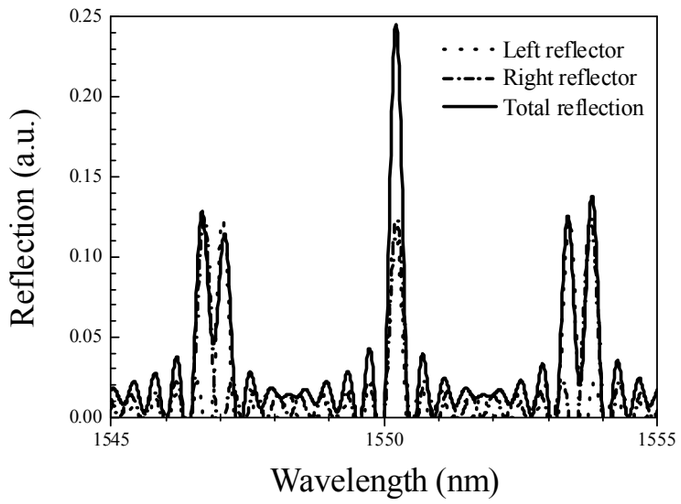

Fig. 6. Vernier tuning showing an overlap of reflection peaks at 1550 nm.

4. Multiple slot lasers

In this section a single section slotted laser with slots etched into the ridge of the waveguide down to the active region is introduced and characterised. This single section laser will form the basics for our three section tunable laser when combined with another similar section and a gain section which provides most of the optical gain. These slotted sections are termed "active slotted mirrors" as there is optical loss from each individual slot and therefore the reflection from a group of slots will saturate quickly if the slot loss is not effectively compensated. In the design presented here, the mirror regions are also actively pumped which provides the necessary gain under current injection to compensate for the loss introduced by the slots.

Firstly the scattering matrix method (SMM) as described earlier to model single slot lasers is used to determine the reflection, transmission, mirror loss and full width at half maximum (FWHM) of the reflection bandwidth profile with wavelength for a number of different slots at a particular slot spacing and gain conditions.

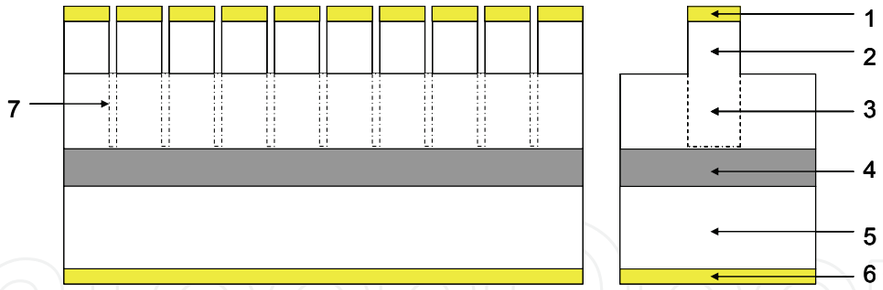

1 = Upper electrically conductive layer, 2 = Ridge of the waveguide, 3 = Upper cladding layer, 4 = Active region, 5 = Lower cladding layer, 6 = Lower electrically conductive layer, 7 = Etched slot.

Fig. 7. Single section slotted laser schematic showing nine etched slots.

A slot spacing of ~ 100 μm is chosen as this provides a reflection spectrum with super-mode peaks at ~ 400 GHz (3.2 nm) spacing. The free spectral range of the super-mode peaks is determined by the slot spacing through the following formula

$$FSR = \frac{\lambda^2}{2n_g L} \tag{11}$$

where n_g is the group effective index, L is the slot spacing and λ is the nominal wavelength. Starting from the SMM to describe a single slot with both slot interfaces straight etched into a medium that has gain and with anti-reflective (AR) coated facets, the reflection amplitude (r_{left}) and transmission amplitude (t_{total}) is determined simply by collecting SMM terms for slot sections and adding AR coated sections with the required slot spacing in between. The calculated power reflection for a single active section slotted laser with AR coated facets for differing numbers of slots is shown in Fig. 8.

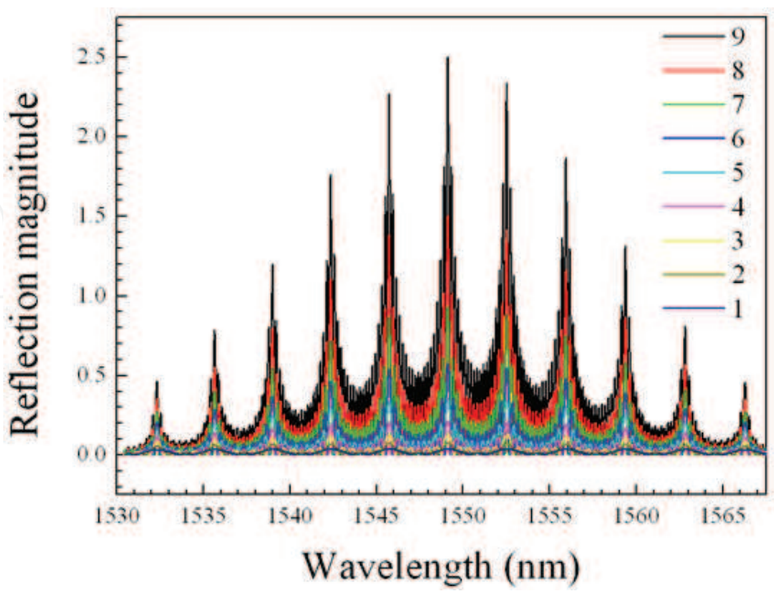

Fig. 8. Calculated power reflection spectrum for a single section active slotted laser with slot numbers form 1 to 9.

From Fig. 8 as the number of slots is increased the reflection at wavelengths determined by the slot spacing is also increased. A power reflection of over 1 is possible as there is considerable gain between the slots. As the mirror loss spectrum is inversely proportional to the reflection spectrum, the wavelength determined by these peaks will reach threshold first and lase at these positions provided the round trip loss is overcome by the gain between the slots. The FWHM of the main reflection peak also changes with slot number and is shown below in Fig. 9.

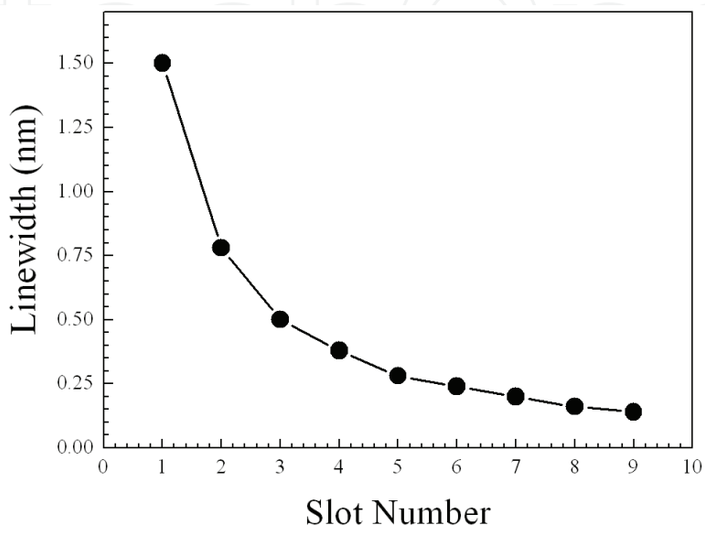

Fig. 9. Reflection linewidth versus slot number.

As the number of slots increases the linewidth of the reflection peaks decreases, therefore less cavity modes are covered by each super-mode meaning less cavity mode jumps are seen in the laser output spectrum. Increasing the number of slots also increases the length of the laser. Therefore a balance needs to be found between the reflection spectrum bandwidth and the laser length as it is better to keep the laser length as small as possible for integration on photonic chips.

As shown in (Lu, Guo et al. 2009) the slot can be described as a discontinuity as only the waveguide to slot interface provides meaningful reflection therefore using the SMM the total amplitude reflection can be approximated by the following formula

$$r = r_S \left[\frac{1 - \left(t_S^2 \exp\left(-2i\beta L\right)\right)^N}{1 - t_S^2 \exp\left(-2i\beta L\right)} \right] \tag{12}$$

where r_s is the slot reflection, t_s is the slot transmission and N is the slot number. The total amplitude transmission can also be approximated to

$$t = t_S \left[\frac{1 - t_S^{N-1} \exp\left(-\left(N-1\right)i\beta L\right)}{1 - t_S \exp\left(-i\beta L\right)} \right] \tag{13}$$

These formulae reduce the complexity of calculating the reflection and transmission of multiple slot laser diodes.

Including a gain section and another nine slot mirror section gives increased tunability using the Vernier effect as described above. A schematic of the laser structure is give in Fig. 10 below.

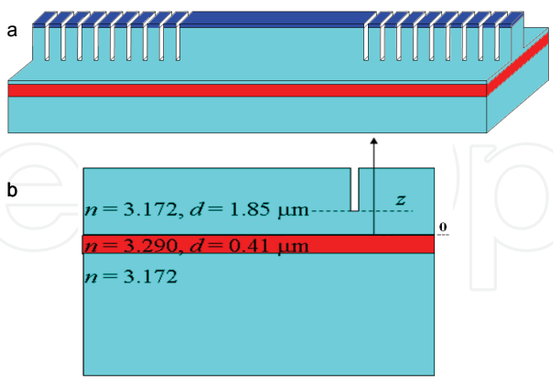

Fig. 10. a - Three section laser schematic showing the presence of etched slots, b – cross section of one slot area showing the slot depth.

Using the SMM to simulate the design shown above with the gain fixed in all sections and the refractive index changed by changing the carrier density in the mirror sections the output wavelength versus both mirror injection currents is found as shown below in Fig. 11.

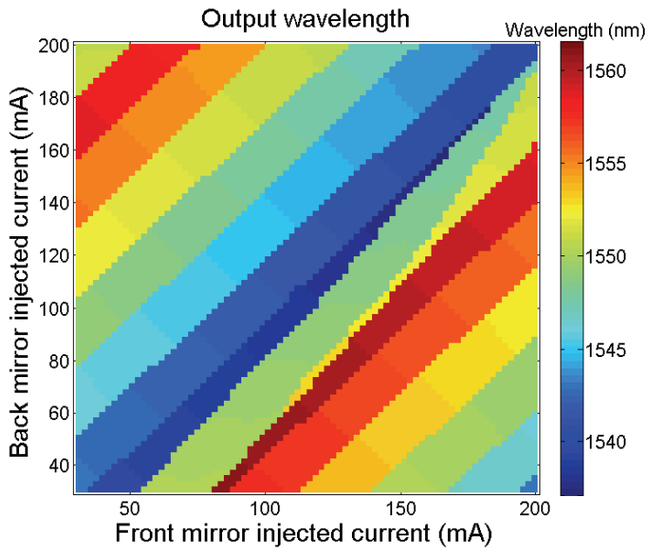

Fig. 11. Simulated three section tunable laser output wavelength versus mirror section injection currents (Gain section is held at a constant injection current).

5. Experimental laser diode characterization

The laser presented here consists of a central gain section of 500 μm and two mirror sections, the back mirror section has nine slots at a slot spacing of 108 μm giving a back mirror section length of 972 μm and the front mirror section which also has nine slots however the slot spacing is 97 μm giving a front mirror section length of 873 μm. The large gain section is chosen to provide sufficient gain as the mirrors have a high loss associated with them. The

total cavity length is ~ 2345 μm and each slot has a length in the propagation direction of ~ 1 μm. By having slightly differing slot spacing in the front and back mirror sections the Vernier tuning mechanism describe above can be used to extend the tuning range greatly. A discrete tuning of 400 GHz is achieved with this slot spacing as with a group index of 3.5 a free spectral range (FSR) of 3.53 nm and 3.17 nm is observed for both front and back mirror reflectors respectively. The laser operates in a similar fashion to a surface grating Bragg reflector laser as reported in (Jayaraman, Chuang et al. 1993), however due to the large distance between the slots (~100 μm) the mirror sections operates as a very high order grating. The large distance between the slots is also beneficial in directly injecting carriers to these regions to produce active mirror sections. The results from two lasers are given here one in which quantum well intermixing (QWI) is used to change the bandgap from 1550 nm to 1500 nm, while the other laser operates at 1550 nm. The tunable laser design described earlier was realized using the same fabrication steps as for a standard ridge waveguide laser. The laser epitaxial structure is a standard design employing an active region of 5 AlGaInAs quantum wells surrounded by InP n- and p-doped cladding regions. 2.5-μm-wide ridge waveguides were formed by inductively coupled plasma etching using Cl_2/N_2 gas. The slots are etched simultaneously with the ridge to a depth just into the waveguide core. The sidewalls are passivated with SiO_2 and an opening is made to the top of the ridge where a patterned Ti/Pt/Au electron-beam-evaporated ohmic contact is formed by lift-off lithography. The etched slot is sufficient to isolate the different longitudinal sections of the device allowing independent current injection. Following thinning of the substrate to 120 μm, an Au/Ge/Ni/Au contact is evaporated on to the n-type substrate. The devices are cleaved to the desired lengths and a single-layer antireflection coating applied to the facets.

To characterise the laser, three independent current sources are used to independently inject current into the gain and two mirror sections of the laser. The first device was mounted on a heat sink and held at a constant temperature of 20° C using a thermoelectric cooling unit. The current injected into the central gain section is fixed at 100 mA. The currents into the front and back mirror sections were scanned between 10 and 100 mA with a step of 1 mA. The wavelength and peak power of the laser emission spectrum and the side-mode-suppression-ratio (SMSR) were recorded using an optical spectrum analyzer with a resolution bandwidth of 0.1 nm. Fig. 12 shows the fibre coupled output power spectra under different current settings. A high SMSR (>30 dB) is required for single mode laser diodes used in optical communications.

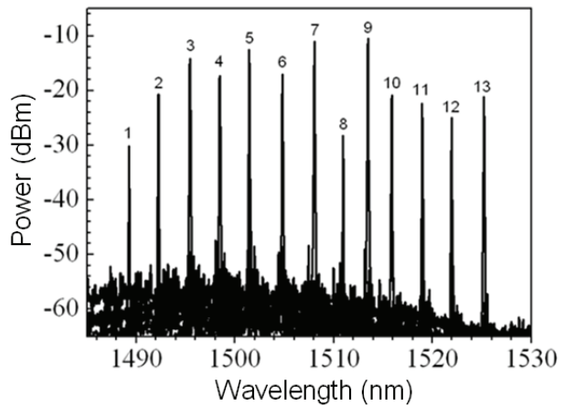

Fig. 12. Fiber coupled output power spectra under different current settings.

Relatively large power variations can be seen mainly because the front mirror current has been changed significantly in the scan in order to fully explore the tuning characteristics of the laser. Fig. 13 shows a diagram of the wavelength peaks and their corresponding SMSRs. A discrete tuning behaviour can be clearly seen over a tuning range of over 30 nm. With this experimental arrangement, a total of 13 discrete wavelengths can be accessed with a wavelength spacing around 3 nm as expected for the present design. 11 of the modes have a SMSR larger than 30 dB, except the 1st and 8th modes whose SMSR is around 20 dB.

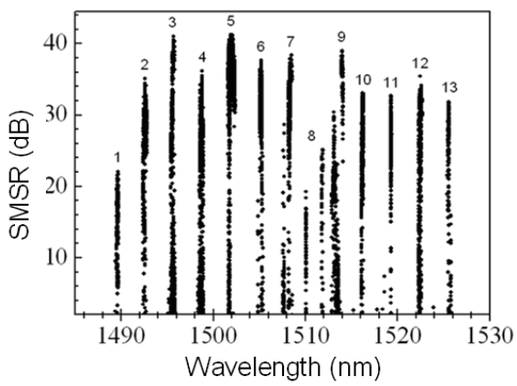

Fig. 13. Three section tunable laser SMSR versus wavelength for different mirror section injection currents.

The second laser described here is similar to the one described above however no QWI is used and therefore the wavelength is tuned around 1550 nm. Fig. 14 shows a wavelength tuning map versus both mirror section injection currents. Discrete mode hopping occurs at the boundaries of each different color section within this map. A total discontinuous tuning range of more than 40 nm is observed. The SMSR map versus both mirror currents is shown in Fig. 15. Clear islands of stable wavelength and high SMSR are observed in the maps.

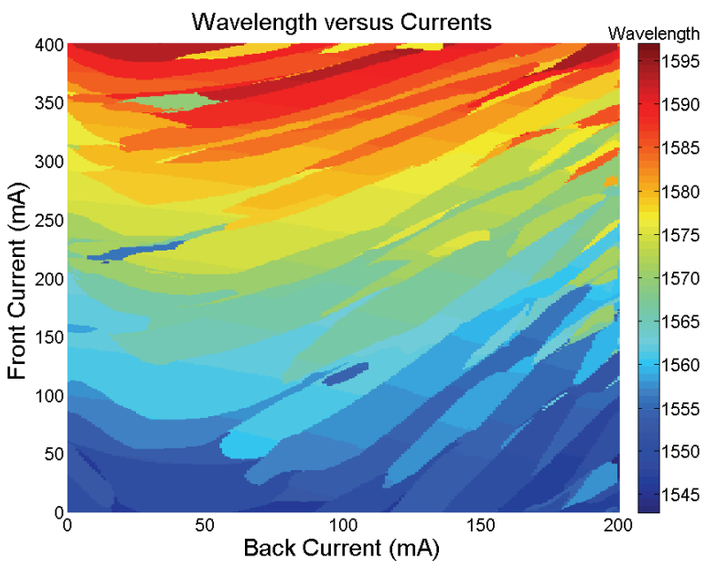

Fig. 14. Wavelength tuning map versus both mirror section injection currents.

The threshold current is difficult to determine accurately as the device has three sections but when both mirror section injection currents are set for a particular mode a threshold current of 56 mA in the gain section is observed. When all three sections are biased together a threshold current of 146 mA is observed.

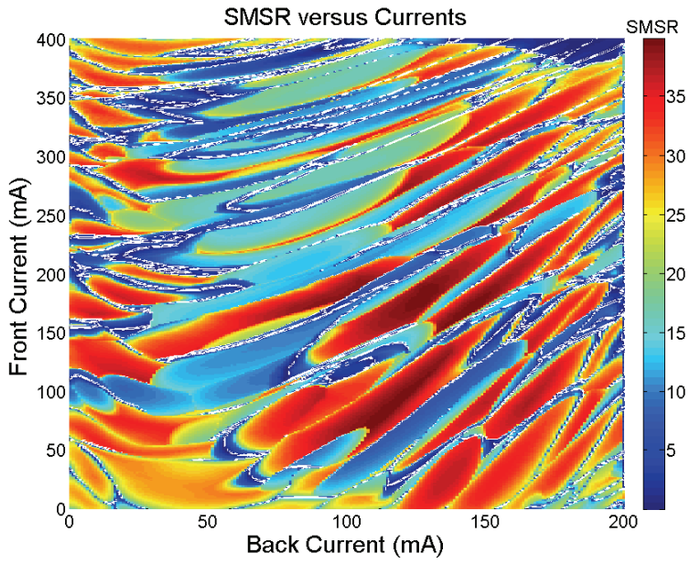

Fig. 15. SMSR tuning map versus both mirror section injection currents.

For comparison a four section sample grated distributed Bragg reflector (SG-DBR) laser wavelength map versus mirror section currents is shown in Fig. 16 below. The SG-DBR is a state of the art semiconductor tunable laser and is used extensively in optical communications and trace gas detection.

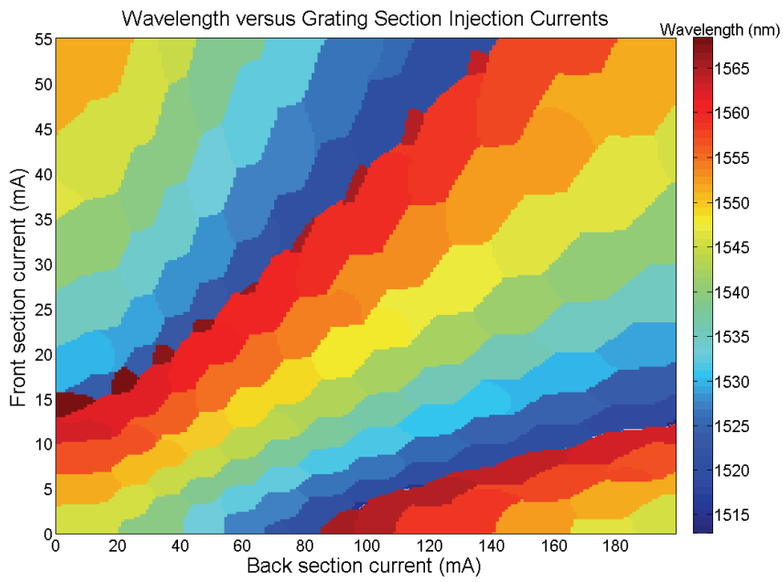

Fig. 16. Wavelength tuning map versus both mirror section injection currents for SG-DBR laser diode.

In order for accurate tuning to the ITU grid the super mode positions need to be fine tuned to a particular wavelength. To do this the laser needs to be continuously tunable over some wavelength range. The continuous tunability of one mode of the laser described above operating around 1550 nm is shown below in Fig. 17. This mode exhibit a continuous tuning range of 1.6 nm which allows for accurate setting of the laser to precise optical frequencies. The continuous tuning of this mode by current injection suggests that full carrier clamping does not take place in the mirror sections of this laser. In comparison, an SGDBR laser has a continuous tuning range of <0.4 nm for all discrete modes which is limited by the longitudinal mode spacing, although its quasi-continuous tuning range is much greater (Oku, Kondo et al. 1998; Mason, Fish et al. 2000).

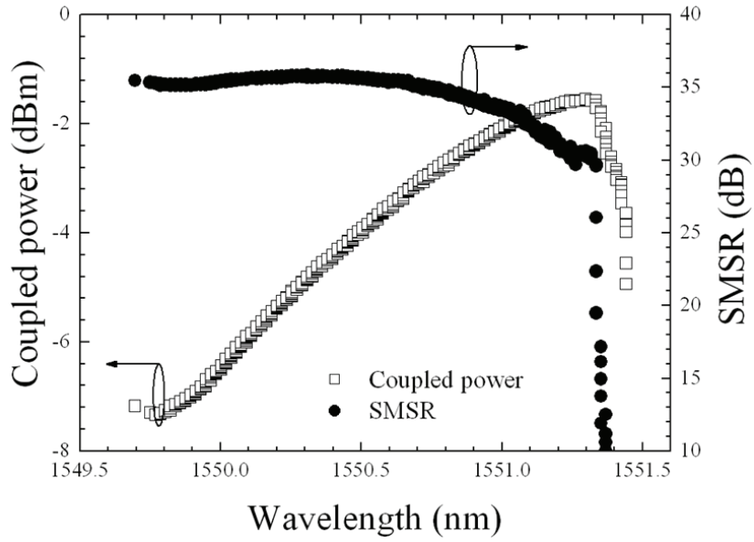

Fig. 17. Measured SMSR versus tuning wavelength due to a linear decrease in both mirror currents

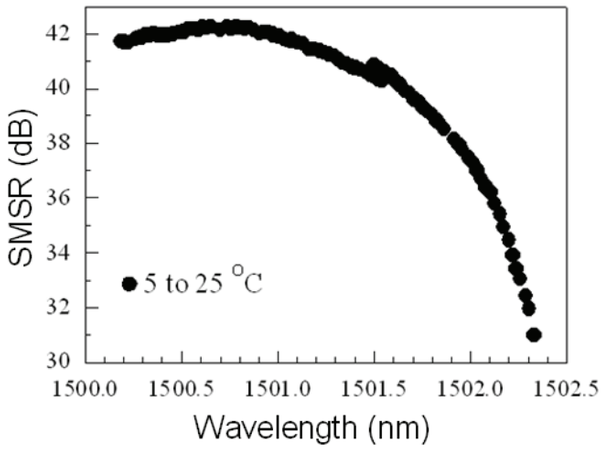

Fig. 18. SMSR versus wavelength for a discrete mode of the QWI laser with change in substrate temperature from 5 to 25° C. The temperature is increased linearly from left to right.

Fig. 18. shows the evolution of the wavelength and the associated SMSR due to thermal effects associated with a change of heat sink temperature from 5 to 25 ^{o}C, here the temperature is varied linearly over this range increasing from left to right in Fig. 17 below. A continuous tuning of over 2 nm while maintaining a SMSR of over 30 dB is measured. The change in wavelength with temperature is in line with the change in the index of InP which is 1.9×10^{-4} /K.

6. Integration of an optical amplifier

In order to demonstrate the compatibility with different photonic components, a semiconductor optical amplifier (SOA) was monolithically integrated with the tuneable laser source. The SOA consists of an 800μm long waveguide section on the output section. The SOA waveguide is curved to meets the output facet at a 5° angle reducing the requirement on the antireflection coating. This method reduces the back reflections to a negligible level. Figure 19 shows seven wavelength channels spaced 400 GHz apart which are accessible by the device. The optical output power is significantly increased by the SOA with channel powers ranging from 10 dBm to 14.2 dBm. All seven channels exhibit a SMSR greater than 30dB with a maximum SMSR of approximately 40dB. No deterioration of the maximum SMSR was observed compared to the laser without the SOA. Figure 20 shows the device output power as a function of the total laser drive current for three different SOA currents. The gain and tuning sections of the laser were connected together for this measurement. The device exhibits an optical output power in excess of 30 mW for a SOA current of 250 mA.

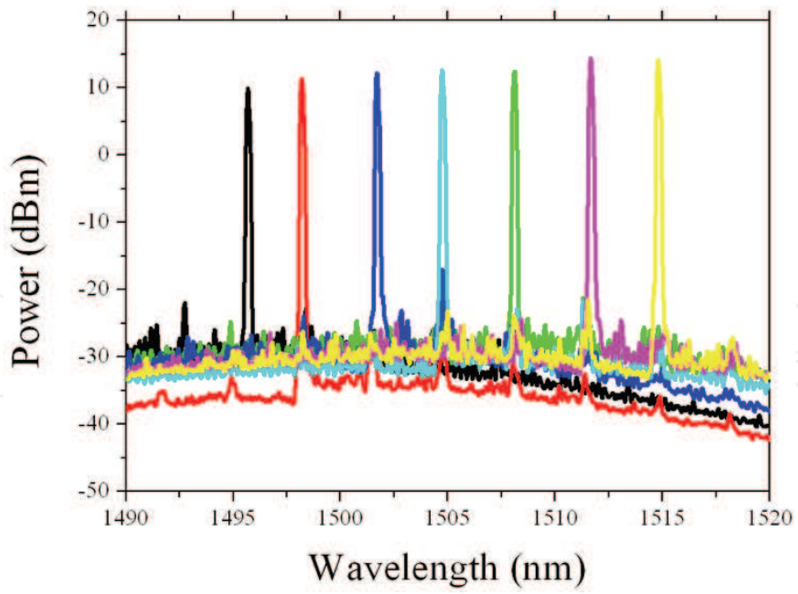

Fig. 19. Seven wavelength channels accessible by the laser integrated with an SOA showing maximum channel power of 14.2 dBm and a maximum SMSR of approx. 40 dB

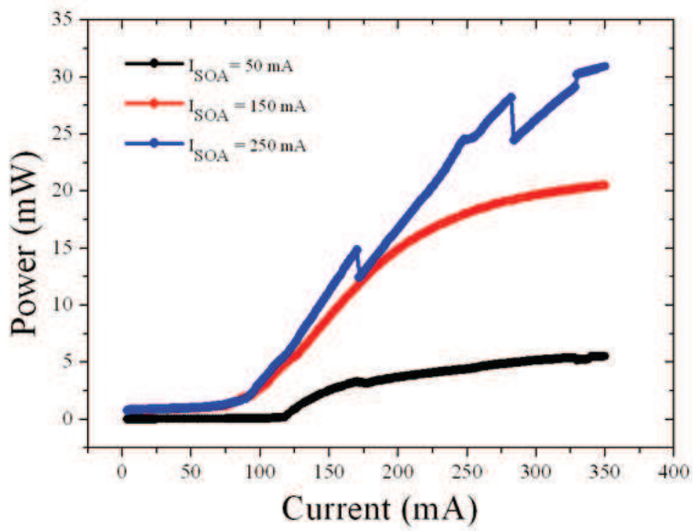

Fig. 20. Optical power as a function of laser drive current for three different SOA currents. The SOA increases the maximum device output power to 30 mW.

The graph shows how increased current injection into the amplifier increases the output power and delays the onset of gain saturation. As the SOA is located adjacent to the mirror section the high SOA drive currents can lead to significant heating of the reflector sections and current leakage into the mirror section. The resulting temperature and current changes cause a slight offset in the front reflector refractive index and a resultant change in the reflectivity spectrum. The blue graph in Fig 20 shows how the output power can change abruptly when the laser performs a mode jump due to thermal and current feedback from the SOA. In a tuneable laser with control over the individual sections, these effects can be offset by readjustment of the reflector currents.

7. Conclusion

The slotted tunable laser described here has many advantages over other state of the art semiconductor tunable laser diodes, however there are also some disadvantages with the slotted tunable laser design.

The key advantages of this laser are:

a. no re-growth step is required during manufacturing
b. no output facet necessary for operation so cleaving is not required
c. highly compatible with integration
d. insensitive to feed-back, therefore may not require optical isolator
e. high switching speed of the order of 1 ns
f. potentially very narrow line-width (of the order of MHz, unconfirmed)

The major advantages of the SFP tunable laser relate to the simpler manufacturing process enabled by the lack of any re-growth step being required. In addition no cleaving is required and this provides its compatibility with integration. This combination should provide an opportunity to obtain high yields with complex integrated devices, such as, a tunable laser, modulator and SOA.

The key disadvantages of this laser are:

a. current devices are significantly longer than competitive lasers, such as, sampled grating distributed Bragg reflector lasers (SG-DBR).
b. current designs have a large channel spacing, of the order of 400 GHz.

The fact that the slotted lasers are longer than competitive lasers reduces the yield advantage of the slotted tunable lasers. However, this should be proportionately less significant in highly integrated devices that include modulators, etc.

Direct comparison with the SG-DBR laser shows that this laser is easier and cheaper to fabricate however it cannot achieve full wavelength coverage of the C or L bands with high SMSR as the SG-DBR can.

One of the most important considerations for a tunable laser is the ability to tune to 50 GHz channel spacing in the C or L band for applications in DWDM applications. In order to address this 50 GHz issue, we are now investigating ways to incorporate a phase section that will allow more continuous tuning. The tunable laser described here also has a major advantage over most other tunable semiconductor lasers as it can be very easily integrated with other photonic components as describe above for integration with a SOA. More work is needed to integrate with Mach-Zehnder modulators and other such photonic devices.

8. Acknowledgements

The authors would like to acknowledge the help received from B. Corbett, J. P. Engelstaedter, B. Roycroft and F. Peters from Tyndall National Institute, Cork, Ireland.

The authors would like to acknowledge the funding received Science Foundation Ireland during the course of this work.

9. References

Buus, J., M.-C. Amann, et al., Eds. (2005). Tunable Laser Diodes and Related Optical Sources, Wiley-IEEE Press.

Coldren, L. and T. Koch (1984). "Analysis and design of coupled-cavity lasers--Part I: Threshold gain analysis and design guidelines." Quantum Electronics, IEEE Journal of 20(6): 659-670.

Coldren, L. A. (2000). "Monolithic tunable diode lasers." Selected Topics in Quantum Electronics, IEEE Journal of 6(6): 988-999.

Corbett, B. and D. McDonald (1995). "Single longitudinal mode ridge waveguide 1.3 micon Fabry-Perot laser by modal perturbation." Electronics Letters 31(25): 2181-2182.

DeChiaro, L. F. (1991). "Spectral width reduction in multilongitudinal mode lasers by spatial loss profiling." Lightwave Technology, Journal of 9(8): 975-986.

Engelstaedter, J. P., B. Roycroft, et al. (2008). "Laser and detector using integrated reflector for photonic integration." Electronics Letters 44(17): 1017-1019.

Fessant, T. and Y. Boucher (1998). "Additional modal selectivity induced by a localized defect in quarter-wave-shifted DFB lasers." Quantum Electronics, IEEE Journal of 34(4): 602-608.

Guo, W. H., L. Qiao-Yin, et al. (2004). "Fourier series expansion method for gain measurement from amplified spontaneous emission spectra of Fabry-Perot semiconductor lasers." Quantum Electronics, IEEE Journal of 40(2): 123-129.

Healy, T., F. C. Garcia Gunning, et al. (2007). "Multi-wavelength source using low drive-voltage amplitude modulators for optical communications." Opt. Express 15(6): 2981-2986.

Jayaraman, V., Z. M. Chuang, et al. (1993). "Theory, design, and performance of extended tuning range semiconductor lasers with sampled gratings." Quantum Electronics, IEEE Journal of 29(6): 1824-1834.

John, P., J. Dewi, et al. (2005). Specifying the wavelength and temperature tuning range of a Fabry-Perot laser containing refractive index perturbations (Invited Paper), SPIE.

Klehr, A., G. Beister, et al. (2001). "Defect recognition via longitudinal mode analysis of high power fundamental mode and broad area edge emitting laser diodes." Journal of Applied Physics 90(1): 43.

Lambkin, P., C. Percival, et al. (2004). "Reflectivity measurements of intracavity defects in laser diodes." Quantum Electronics, IEEE Journal of 40(1): 10-17.

Lu, Q. Y., W. H. Guo, et al. (2009). "Analysis of leaky modes in deep-ridge waveguides using the compact 2D FDTD method." Electronics Letters 45(13): 700-701.

Mason, B., G. A. Fish, et al. (2000). Characteristics of sampled grating DBR lasers with integrated semiconductor optical amplifiers. Optical Fiber Communication Conference, 2000.

McDonald, D. and B. Corbett (1996). "Performance characteristics of quasi-single longitudinal-mode Fabry-Perot lasers." Photonics Technology Letters, IEEE 8(9): 1127-1129.

O'Brien, S. and E. P. O'Reilly (2005). "Theory of improved spectral purity in index patterned Fabry-Perot lasers." Applied Physics Letters 86(20): N.PAG.

Oku, S., S. Kondo, et al. (1998). Surface-grating Bragg reflector lasers using deeply etched groove formed by reactive beam etching. Indium Phosphide and Related Materials, 1998 International Conference on.

Peters, F. H. and D. T. Cassidy (1991). "Model of the spectral output of gain-guided and index-guided semiconductor diode lasers." J. Opt. Soc. Am. B 8(1): 99-105.

Phelan, R., M. Lynch, et al. (2005). "Simultaneous multispecies gas sensing by use of a sampled grating distributed Bragg reflector and modulated grating Y laser diode." Appl. Opt. 44(27): 5824-5831.

Phelan, R., G. Wei-Hua, et al. (2008). "A Novel Two-Section Tunable Discrete Mode Fabry-Perot Laser Exhibiting Nanosecond Wavelength Switching." Quantum Electronics, IEEE Journal of 44(4): 331-337.

Raring, J. W. and L. A. Coldren (2007). "40-Gb/s Widely Tunable Transceivers." Selected Topics in Quantum Electronics, IEEE Journal of 13(1): 3-14.

Rigole, P. J., S. Nilsson, et al. (1995). "114-nm wavelength tuning range of a vertical grating assisted codirectional coupler laser with a super structure grating distributed Bragg reflector." Photonics Technology Letters, IEEE 7(7): 697-699.

Roycroft, B., P. Lambkin, et al. (2007). "Transition From Perturbed to Coupled-Cavity Behavior With Asymmetric Spectral Emission in Ridge Lasers Emitting at 1.55 μm." Photonics Technology Letters, IEEE 19(2): 58-60.

Ward, A. J., D. J. Robbins, et al. (2005). "Widely tunable DS-DBR laser with monolithically integrated SOA: design and performance." Selected Topics in Quantum Electronics, IEEE Journal of 11(1): 149-156.

Welch, D. F., F. A. Kish, et al. (2006). "The Realization of Large-Scale Photonic Integrated Circuits and the Associated Impact on Fiber-Optic Communication Systems." J. Lightwave Technol. 24(12): 4674-4683.

IntechOpen

IntechOpen

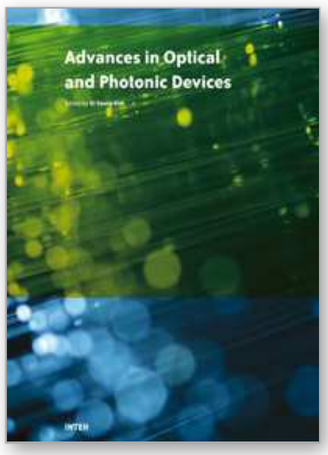

Advances in Optical and Photonic Devices

Edited by Ki Young Kim

ISBN 978-953-7619-76-3
Hard cover, 352 pages
Publisher InTech
Published online 01, January, 2010
Published in print edition January, 2010

The title of this book, Advances in Optical and Photonic Devices, encompasses a broad range of theory and applications which are of interest for diverse classes of optical and photonic devices. Unquestionably, recent successful achievements in modern optical communications and multifunctional systems have been accomplished based on composing “building blocks” of a variety of optical and photonic devices. Thus, the grasp of current trends and needs in device technology would be useful for further development of such a range of relative applications. The book is going to be a collection of contemporary researches and developments of various devices and structures in the area of optics and photonics. It is composed of 17 excellent chapters covering fundamental theory, physical operation mechanisms, fabrication and measurement techniques, and application examples. Besides, it contains comprehensive reviews of recent trends and advancements in the field. First six chapters are especially focused on diverse aspects of recent developments of lasers and related technologies, while the later chapters deal with various optical and photonic devices including waveguides, filters, oscillators, isolators, photodiodes, photomultipliers, microcavities, and so on. Although the book is a collected edition of specific technological issues, I strongly believe that the readers can obtain generous and overall ideas and knowledge of the state-of-the-art technologies in optical and photonic devices. Lastly, special words of thanks should go to all the scientists and engineers who have devoted a great deal of time to writing excellent chapters in this book.

How to reference

In order to correctly reference this scholarly work, feel free to copy and paste the following:

D. C. Byrne, W. H. Guo, Q. Lu and J. F. Donegan (2010). A Tunable Semiconductor Lased Based on Etched Slots Suitable for Monolithic Integration, Advances in Optical and Photonic Devices, Ki Young Kim (Ed.), ISBN: 978-953-7619-76-3, InTech, Available from: http://www.intechopen.com/books/advances-in-optical-and-photonic-devices/a-tunable-semiconductor-lased-based-on-etched-slots-suitable-for-monolithic-integration

INTECH
open science | open minds

InTech Europe
University Campus STeP Ri
Slavka Krautzeka 83/A
51000 Rijeka, Croatia
Phone: +385 (51) 770 447

InTech China
Unit 405, Office Block, Hotel Equatorial Shanghai
No.65, Yan An Road (West), Shanghai, 200040, China
中国上海市延安西路65号上海国际贵都大饭店办公楼405单元
Phone: +86-21-62489820

Fax: +385 (51) 686 166
www.intechopen.com

Fax: +86-21-62489821

IntechOpen

IntechOpen

© 2010 The Author(s). Licensee IntechOpen. This chapter is distributed under the terms of the Creative Commons Attribution-NonCommercial-ShareAlike-3.0 License, which permits use, distribution and reproduction for non-commercial purposes, provided the original is properly cited and derivative works building on this content are distributed under the same license.

IntechOpen

IntechOpen